

1 **Versatile Cell-Based Assay for Measuring Base Excision Repair of DNA Alkylation**  
2 **Damage**

3

4 Yong Li<sup>1</sup>, Peng Mao<sup>2,6</sup>, Evelina Y. Basenko<sup>5,7</sup>, Zachary Lewis<sup>3,4,5</sup>, Michael Smerdon<sup>2</sup>, Wioletta  
5 Czaja\*<sup>1,2,8</sup>

6

7 <sup>1</sup> The Hormel Institute, University of Minnesota, Austin, Minnesota, 55912, USA. (current  
8 address)

9 <sup>2</sup> School of Molecular Biosciences, Washington State University, Pullman, Washington 99164,  
10 USA.

11 <sup>3</sup> Department of Microbiology, University of Georgia, Athens, Georgia, 30602, USA.

12 <sup>4</sup> Department of Plant Biology, University of Georgia, Athens, GA, 30602, USA.

13

14 <sup>5</sup> Department of Genetics, University of Georgia, Athens, GA, 30602, USA.

15

16 <sup>6</sup> Comprehensive Cancer Center, University of New Mexico, Albuquerque, NM, 87131, USA.  
17 (current address)

18

19 <sup>7</sup> Department of Biochemistry and Systems Biology, University of Liverpool, Liverpool L69 3BX,  
20 United Kingdom. (current address)

21

22 <sup>8</sup> Department of Biochemistry and Molecular Biology, University of Georgia, Athens, Georgia,  
23 30602, USA.

24

25

26

27 \*Address for correspondence

28 Wioletta Czaja  
29 The Hormel Institute  
30 University of Minnesota  
31 Austin, Minnesota, 55912, USA  
32 Email: [wczaja@umn.edu](mailto:wczaja@umn.edu)  
33

34

35 **Abstract**

36 DNA alkylation damage induced by environmental carcinogens, chemotherapy drugs, or  
37 endogenous metabolites plays a central role in mutagenesis, carcinogenesis, and cancer  
38 therapy. Base excision repair (BER) is a conserved, front line DNA repair pathway that removes  
39 alkylation damage from DNA. The capacity of BER to repair DNA alkylation varies markedly  
40 between different cell types and tissues, which correlates with cancer risk and cellular  
41 responses to alkylation chemotherapy. The ability to measure cellular rates of alkylation  
42 damage repair by the BER pathway is critically important for better understanding of the  
43 fundamental processes involved in carcinogenesis, and also to advance development of new  
44 therapeutic strategies. Methods for assessing the rates of alkylation damage and repair,  
45 especially in human cells, are limited, prone to significant variability due to the unstable nature  
46 of some of the alkyl adducts, and often rely on indirect measurements of BER activity. Here, we  
47 report a highly reproducible and quantitative, cell-based assay, named alk-BER (alkylation Base  
48 Excision Repair) for measuring rates of BER following alkylation DNA damage. The alk-BER  
49 assay involves specific detection of methyl DNA adducts (7-methyl guanine and 3-methyl  
50 adenine) directly in genomic DNA. The assay has been developed and adapted to measure the  
51 activity of BER in fungal model systems and human cell lines. Considering the specificity and  
52 conserved nature of BER enzymes, the assay can be adapted to virtually any type of cultured  
53 cells. Alk-BER offers a cost efficient and reliable method that can effectively complement  
54 existing approaches to advance integrative research on mechanisms of alkylation DNA damage  
55 and repair.

56

57

58

59

60

61

62

63 **Key words:** Alkylated DNA damage, alkylating agents, DNA methylation, base excision repair,  
64 DNA repair capacity, DNA damage quantitation

## 65 1. Introduction

66 DNA alkylation induced by methylating agents such as environmental carcinogens (e.g.,  
67 smoke), by-products of cellular metabolism (e.g., methyl group donor S-adenosyl methionine),  
68 or chemotherapy drugs (e.g., temozolomide, procarbazine) represents one of the most  
69 abundant types of DNA base damage that forms in human cells. Monofunctional alkylating  
70 agents, like methyl methanesulfonate (MMS) or the anticancer drug temozolomide (TMZ) induce  
71 formation of N-methyl and O-methyl DNA adducts such as N7-methylguanine (7meG), N3-  
72 methyladenine (3meA) and O6-methylguanine (O6meG) [1, 2]. Methyl DNA adducts (MDAs)  
73 have cytotoxic and mutagenic properties because of their ability to block gene transcription and  
74 interfere with the fidelity of DNA replication. Persistent and inefficiently repaired methyl DNA  
75 adducts can induce microsatellite instability, frameshift mutations, and G→A transition  
76 mutations, that are commonly found in genes critical for malignant transformation, including the  
77 *H-ras* oncogene or *TP53* tumor suppressor gene [3-5]. Despite their carcinogenic properties,  
78 DNA alkylating agents, such as dacarbazine, temozolomide and streptozotin, have been used  
79 for decades in treating various cancers, including melanoma, glioma, and lymphoma [2, 6, 7].  
80 Therapy with alkylating agents can be effective; however, these agents are extremely toxic and  
81 prolonged treatment often leads to chemoresistance and formation of secondary cancers [8, 9].  
82 Human responses to alkylating agents vary considerably between individuals, which highlights  
83 the involvement of genetic and epigenetic mechanisms in the modulation of cellular toxicity to  
84 alkylating agents [2, 10, 11].

85 Base excision repair (BER) is the primary pathway involved in the removal of alkylation DNA  
86 damage induced by methylating agents [2, 12, 13]. Repair of methyl DNA adducts through the  
87 BER pathway is accomplished in four sequential steps, each carried out by a specific group of  
88 enzymes [14]. The first step is catalyzed by DNA glycosylases (e.g., AAG), which specifically  
89 recognize and bind to a damaged base, and subsequently catalyze cleavage of the glycosidic  
90 bond between the damaged base and DNA backbone [15, 16]. This reaction results in the  
91 release of the damaged base from DNA, and the formation of abasic AP (apurinic/apyrimidinic)  
92 sites. The second step involves incision of the DNA backbone 5' upstream of the AP sites by AP  
93 endonucleases (e.g., APE1), which results in the formation of single strand DNA breaks (SSBs)  
94 [17, 18]. In mammalian cells, AP sites and SSBs are recognized by poly ADP-ribose  
95 polymerase 1 (PARP1) [19, 20]. Activated PARP1 catalyzes the formation of ADP-ribose  
96 chains, which serve as a docking platform that facilitates recruitment and assembly of the  
97 multiprotein BER complex (XRCC1-POL $\beta$ -LIG3). Breaks in DNA are filled in by DNA  
98 polymerases (primarily POL $\beta$ ) using the undamaged complementary DNA strand as a template

99 [21]. Nicks in the damaged strand are sealed by ligases (e.g., LIG3), which finalizes repair of the  
100 damaged DNA strand [22, 23].

101 Importantly, methylation-derived repair intermediates such as AP sites and SSBs are highly  
102 cytotoxic and mutagenic. Therefore, individual steps in the BER pathway need to be tightly  
103 regulated and coordinated to prevent accumulation of those intermediates, cell death,  
104 mutagenesis, and carcinogenesis [2, 24]. Genetic studies in yeast, mouse models, and human  
105 cells have demonstrated that loss of the tight coordination between individual steps in the BER  
106 pathway can trigger genome instability, increased mutagenesis, or cell death [2, 5, 24-27].  
107 Levels and activities of BER proteins vary significantly between cells, tissues, and individuals  
108 and correlate with cancer risk and response to alkylation chemotherapy [2, 10, 11, 25, 28-32].  
109 Therefore, measuring and understanding differences in the rate of BER upon alkylation DNA  
110 damage could contribute to the development of new approaches in personalized disease  
111 prevention and treatment.

112 The BER pathway is dysregulated in many cancers and is often associated with cancer  
113 heterogeneity, metastasis, and chemoresistance. Pharmacological inhibition of BER with PARP  
114 inhibitors (e.g., olaparib) has shown enhanced cytotoxicity of various anticancer agents,  
115 especially in tumors with defects in homologous recombination [33-37]. Identifying a pre-existing  
116 BER imbalance within a tumor may be highly relevant for determining whether therapy involving  
117 PARP inhibitors and alkylating agents can be beneficial.

118 Quantitation of DNA adduct formation and repair has greatly advanced our understanding of  
119 DNA repair processes. A number of methods have been developed for quantitative analysis of  
120 various enzymatic steps and the overall capacity of BER to repair alkylation DNA damage. The  
121 most sensitive methods for detection and quantitation of alkyl DNA adducts include HPLC/<sup>32</sup>P-  
122 postlabeling, mass spectrometry-based adductomics, and radiolabeling [38-41]. These methods  
123 offer high sensitivity; however, they require specialized equipment, expertise, and complex  
124 sample preparation, which hinders the convenient use of those approaches to investigate  
125 cellular BER mechanisms.

126 The most commonly used cell-based methods to investigate BER, include comet assays  
127 and host cell reactivation (HCR) assays. The comet assay is a single-cell electrophoresis  
128 technique that can be used to assess the capacity of BER to repair alkylation DNA damage  
129 when performed under alkaline conditions [42]. This assay can be used to analyze total levels of  
130 BER repair intermediates, such as alkali labile sites (e.g., abasic sites) and single strand breaks;  
131 however, it does not quantitatively distinguish between these intermediates. The standard  
132 comet assay may not reliably detect persistent and intact base modifications (e.g., 7meG or

133 3meA) that are not converted to AP sites or SSBs. In addition, the comet assay may not detect  
134 lesions that form and persist within highly inaccessible heterochromatin fractions of the genome.  
135 Furthermore, the standard comet assay workflow is laborious and prone to day-to-day  
136 variability. It may also require extensive optimization of experimental conditions, including pH or  
137 salts used during the alkaline electrophoresis steps, to achieve sensitivity and consistent  
138 reproducibility [42, 43]. HCR is another method that has been used to measure the capacity of  
139 BER to repair alkylation DNA damage in living cells [44, 45]. HCR relies on the transfection of  
140 the non-replicating DNA plasmid with a reporter gene (e.g., *luciferase*) that contains chemically-  
141 induced DNA base damage, which is subject to repair by the BER pathway. The presence of the  
142 DNA base damage within the reporter gene inhibits its expression, whereas the repair of base  
143 damage re-activates reporter expression. The HCR assay can be especially challenging to  
144 assess repair of alkylation DNA damage, due to *in vitro* instability of the alkyl DNA adducts (e.g.,  
145 7meG and 3meA), which can markedly affect assay reproducibility [45]. Also, HCR involves a  
146 non-genomic DNA substrate that does not necessarily reflect the complexity of the genomic  
147 chromatin environment.

148 More recently, high resolution, high throughput approaches such as LAF-seq (Lesion-  
149 Adjoining Fragment Sequencing) or NMP-seq (N-methyl purine sequencing) utilizing next  
150 generation DNA sequencing have been developed to enable precise mapping and quantitation  
151 of methyl DNA adducts across the genome, and at specific genomic loci [46, 47]. These  
152 approaches offer unprecedented single base resolution, but can be laborious, involving  
153 generation of DNA sequencing libraries and extensive bioinformatics analyses of the  
154 sequencing data, especially when used with human cells. In addition, those methods may  
155 require high (non-physiological) doses of DNA damaging agents and large amounts of input  
156 DNA.

157 Here we report a reliable, gel-based method, called alk-BER, that offers a fast and  
158 quantitative measure of BER capacity in living cells. Alk-BER was developed by an adaptation  
159 of a previous method for DNA damage quantitation by alkaline gel electrophoresis, originally  
160 developed by Sutherland et al. [48]. Alk-BER can be used to assess overall capacity of BER to  
161 repair MMS-induced alkylation DNA damage within the genome of living cells. The assay can be  
162 used to facilitate identification of new, conserved regulators of the BER pathway by using  
163 complementary model eukaryotic systems, including fungal model organisms and human cells.  
164 Application of the alk-BER assay could also facilitate identification of BER-deficient cancer sub-  
165 types, which might represent suitable targets for therapy with alkylating agents and/or PARP  
166 inhibitors.

167

## 168 **2. Materials and Methods**

169 **2.1. DNA damage and time course of repair in yeast cells.** Yeast (*S. cerevisiae*) liquid cell  
170 cultures were inoculated from single colonies and grown in 10 ml of YPD (Yeast extract -  
171 Peptone-Dextrose) medium for ~ 16 h at 30°C in an orbital shaker. The following day, cells were  
172 sub-cultured in fresh media and grown until the cultures reached the logarithmic stage of  
173 growth, as determined by measuring the optical density of the cell culture (e.g., OD<sub>600</sub> ~ 0.6).  
174 Next, MMS was added to the liquid cultures at a final concentration of 20mM and cells were  
175 incubated for 10 min at 30°C in an orbital shaker. Alternatively, cells were treated with 3.5mM  
176 MMS for 1- 3 h, followed by removal of media containing MMS and repair time course in fresh  
177 media for 1-6 h. Cells were then harvested by centrifugation, and the supernatant fractions  
178 containing MMS were removed and disposed following DEHS guidelines. Cell pellets were  
179 washed with ice-cold phosphate buffered saline (1X PBS), re-suspended in a pre-warmed YPD  
180 media, and allowed to repair for a total of 3 h. Extended repair time points (longer than 4-5  
181 hours) were avoided to ensure that restoration of the genome integrity was due to the activity of  
182 BER, and not due to lesion bypass and DNA replication. Cultures were incubated with  
183 continuous shaking and cell aliquots were collected at different repair time points [49, 50].

184

185 **2.2. Yeast genomic DNA isolation.** Yeast genomic DNA was extracted with the glass bead  
186 method following previously established protocols [51]. Briefly, cell pellets were mixed with 250  
187 µL of DNA lysis buffer [2% (vol/vol) Triton X-100, 1% SDS, 100 mM NaCl, 10 mM Tris-HCl, pH  
188 8.0, 1 mM EDTA, 250 µL of PCI (phenol: chloroform: isoamyl alcohol = 25:24:1), and 150 µL of  
189 acid-washed glass beads, and vortexed vigorously for 4 min. Next, 200 µL of 1xTE buffer (10  
190 mM Tris-HCl, pH 7.5, 1 mM EDTA) were added and cell lysates were centrifuged at 14,000 rpm  
191 at 4°C. The supernatant fraction was transferred to a fresh Eppendorf tube and mixed with 1 mL  
192 of ice-cold 200 proof ethanol. Samples were incubated at -80°C for 15 min to facilitate formation  
193 of the DNA precipitate. Next, samples were centrifuged at 14,000 rpm at 4°C, and washed with  
194 70% (vol/vol) ethanol. The DNA pellets were dissolved in 200 µL of 1xTE buffer and incubated  
195 with 2 µL of RNase A (Thermo Fisher Scientific, cat # EN0531) at 37°C for 1 h to remove RNA.  
196 DNA was subsequently ethanol-precipitated, dissolved in sterile deionized H<sub>2</sub>O, and then stored  
197 at -80°C.

198

199 **2.3. AAG and APE1 reactions.** Purified genomic DNA was processed with (+) or without (-) an  
200 enzymatic cocktail composed of AAG (New England BioLabs, cat# M0313S) and APE1 (New

201 England BioLabs, cat# M0282), to convert MMS-induced 7meG and 3meA to SSBs. DNA  
202 samples (0.6-1µg) were incubated with 1 µL of AAG and 1 µL of APE1 in the reaction buffer (70  
203 mM MOPS, pH 7.5, 1 mM dithiothreitol (DTT), 1 mM EDTA, 5% glycerol) at 37°C for 1 h in a  
204 total reaction volume of 20 µL [52]. Methylated bases were cleaved by AAG glycosylase and the  
205 resulting abasic sites were cleaved by APE1 endonuclease. The reactions were stopped by  
206 adding DNA loading buffer (50 mM NaOH, 1 mM EDTA, 3% Ficoll, 0.025% Bromocresol green,  
207 0.041% Xylene cyanol). Following enzymatic digestion of DNA cleavage products, single and  
208 double strand breaks were resolved on 1.2% alkaline agarose gels and stained with SYBR Gold  
209 [49, 50].

210  
211 **2.4. Alkaline agarose gel electrophoresis.** Alkaline agarose gel electrophoresis was  
212 performed following previously published protocols with modifications [48, 53]. The large gel  
213 electrophoresis box and casting tray were used. The agarose solution was prepared by adding  
214 4.3 g of agarose to 360 ml of H<sub>2</sub>O in a 1 L Erlenmeyer flask and then heating in a microwave  
215 oven until the agarose was dissolved. The solution was cooled to 55°C and then followed by  
216 addition of a 0.1 volume (40ml) of 10X alkaline agarose gel electrophoresis buffer (500 mM  
217 NaOH, 10 mM EDTA, pH 8.0). Addition of 10x alkaline buffer to a hot agarose solution should  
218 be avoided because NaOH in the buffer may cause hydrolysis of the agar. The agarose solution  
219 was poured into a large gel casting tray. After the gel was completely solidified, it was mounted  
220 in the electrophoresis tank. Then the tank was filled with 1X alkaline electrophoresis buffer until  
221 the gel was covered with the buffer at a depth of 3-5 mm above the gel. DNA samples after  
222 AAG and APE1 digestion were collected and 6X alkaline gel-loading buffer (300 mM NaOH, 6  
223 mM EDTA, 18% Ficoll, 0.15% Bromocresol green, 0.25% Xylene cyanol) was added to each  
224 sample. Chelating all Mg<sup>2+</sup> with EDTA (component of the 6X alkaline gel-loading buffer) is  
225 important before loading the samples onto the alkaline agarose gel because in solutions with a  
226 high pH, Mg<sup>2+</sup> can form insoluble Mg (OH)<sub>2</sub> precipitates that entrap DNA and inhibit DNA  
227 mobility through the gel. Samples were loaded and the gel was run at room temperature at 30V  
228 for 19-24 h. Alternatively, the electrophoresis can be run at 4°C in a cold room. We found that  
229 running the gel in a cold room helped improve the sharpness of the DNA bands. Note that after  
230 the run is completed, the Bromocresol green dye may not be visible because of dye diffusion in  
231 the gel. The gel was transferred to a large plexiglass tray, covered with neutralizing solution (1  
232 M Tris-HCl, 1.5M NaCl), and incubated for 30 min with gentle shaking on an orbital shaker. Next  
233 the gel was transferred to staining solution (1x TAE buffer with SYBR gold) and stained for 1 h  
234 with gentle shaking. The container with the gel was covered with aluminum foil to protect the

235 staining solution from light. Following staining, the gel was rinsed and de-stained with H<sub>2</sub>O for 30  
236 min with gentle shaking. An image of the gel was acquired using the Storm phosphor imager.

237

## 238 **2.5. Quantitative analysis of DNA damage and repair following MMS treatment.**

239 Quantitation of methylated bases in genomic DNA was performed on phosphor image data by  
240 using ImageQuant software (Molecular Dynamics) and number-average DNA length analysis.  
241 The number-average length of genomic DNA ( $\pm$  AAG/APE treatment) was used to calculate the  
242 average number of SSBs/kb, and the percentage of MDAs removed (% repair) was determined  
243 as described previously [49, 51]. Briefly, using the ImageQuant software functions, each data  
244 point on the gel image is marked with a box encompassing the entire length of the lane to give  
245 the total area of each lane. The data point corresponding to 1/2 the total area, designated as  
246  $X_{med}$ , is then determined. The  $X_{med}$  value indicates the median migration distance of the DNA  
247 fragments.  $X_{med}$  is converted to the median length  $L_{med}$  of DNA molecules by using a standard  
248 curve generated from the migration of DNA-size markers. The number average molecular  
249 length,  $L_n$ , is calculated from  $L_{med}$  by using the equation  $L_n = 0.6 L_{med}$  [54], assuming a Poisson  
250 distribution of DNA fragments. Numbers of SSBs/kb is calculated using the following equation;  
251  $SSBs/kb = 1/L_n (+AAG+APE1) - 1/L_n (-AAG-APE1)$ . Calculated numbers of SSBs per kb DNA  
252 fragment indicate numbers of MDAs.

253

## 254 **2.6. DNA damage and time course of repair in multicellular fungus *Neurospora crassa*.**

255 Liquid cultures of *N. crassa* were grown for 11 h in VMM (Vogel's minimal medium) media in an  
256 orbital shaker at 30°C. MMS was added to liquid cultures at a final concentration of 3.5mM.  
257 Cells were incubated in the presence of MMS for 3 h. Next, the cells were collected by using a  
258 Buchner funnel, and washed with 500 ml of VMM media to remove MMS. Washed cells were  
259 transferred to pre-warmed VMM media and then allowed to grow at 30°C for 4 h to enable repair  
260 of damaged DNA. Aliquots of cells were harvested and immediately frozen in liquid nitrogen.  
261 Genomic DNA was isolated and 300 ng of genomic DNA was digested with APE1 endonuclease  
262 (cat # M0282S, New England Biolabs), AAG glycosylase (cat # M0313S, New England Biolabs),  
263 or both enzymes in MOPS reaction buffer (70 mM MOPS, pH 7.5, 1 mM dithiothreitol DTT, 1 mM  
264 EDTA, 5% glycerol) for 1 h and 15 min at 37°C. Reactions were stopped by adding alkaline  
265 DNA loading buffer (50 mM NaOH, 1 mM EDTA, 3% Ficoll). Samples were resolved on a 1.2%  
266 alkaline agarose gel. Agarose gels were run in a cold room at 25V for 17 h and then incubated  
267 in neutralization buffer (1.5 M NaCl, 1 M Tris-Cl pH 7.6) for 45 min before being stained with



268 SYBR Gold (cat # S-11494, Life Technologies) for 40 min and de-stained for 30 min before  
269 imaging [55].

270

271 **2.7. DNA damage and time course of repair in human cells.** Human adrenal carcinoma cells  
272 (SW13) were cultured in DMEM (Sigma, cat# D5796) supplemented with 10% fetal bovine  
273 serum FBS (Gibco, cat# 26140-079). Human fibroblast CHON-002, leukemia HAP1, and  
274 lymphoblastoid cells GM12878 were cultured according the ATCC guidelines. Cell cultures were  
275 routinely tested for mycoplasma by using a mycoplasma detection kit (ATCC, cat# 30-1012K).  
276 Cell doubling time was determined following ATCC guidelines and viability was routinely  
277 monitored with trypan blue. Cells were seeded in T25 flasks (~500,000 cells per dish) and  
278 grown for 16-24 h until cells reached 60-70% confluence. One T25 flask was set for each data  
279 point to be collected. In DNA damage dose response experiments SW13 cells were treated with  
280 (0- 20mM) MMS in 1xPBS for 10 min at RT. In DNA damage and repair experiments, SW13  
281 cells were treated with 10 mM (0.1%) MMS for 10 min in 1xPBS at RT, or alternatively ice-cold,  
282 serum-free media can be also used for MMS treatments. Ice-cold treatment is used to inhibit  
283 endogenous background BER during the MMS treatment. MMS was removed and cells were  
284 washed with 1XPBS. Next, fresh pre-warmed media were added and cells were allowed to  
285 repair for 0, 3, 8, or 22 hours. GM 12878 cells were treated with 5mM (0.05%) MMS for 5 min.  
286 Total genomic DNA was purified from each time point using the PureLink genomic DNA mini kit  
287 (K 182001, Thermo Fisher Scientific). DNA was processed with AAG and APE1 enzymes as  
288 described above. DNA was resolved on a 1.2% alkaline agarose gel, run at 30V for 22 h,  
289 stained with SYBR gold, and quantified as described above.

290

## 291 **2.8. Western Blotting**

292 HAP1, SW13 and CHON-002 cells were harvested and frozen at  $-80^{\circ}\text{C}$ . Protein extracts were  
293 prepared in a RIPA buffer (Santa Cruz, sc-24948) plus phosphatase inhibitor (Santa Cruz, sc-  
294 45044 and sc-45044) and equal amounts of protein were separated on TGX stain-free (Bio-Rad,  
295 cat#5678083). Proteins were transferred onto TransBlot LF PVDF (Bio-Rad) and analyzed by  
296 Western blotting using antibodies recognizing the following proteins: AAG (Abcam ab155092,  
297 42KD, 1:5000), beta-actin (Sigma A5441, 33KD, 1:5000).

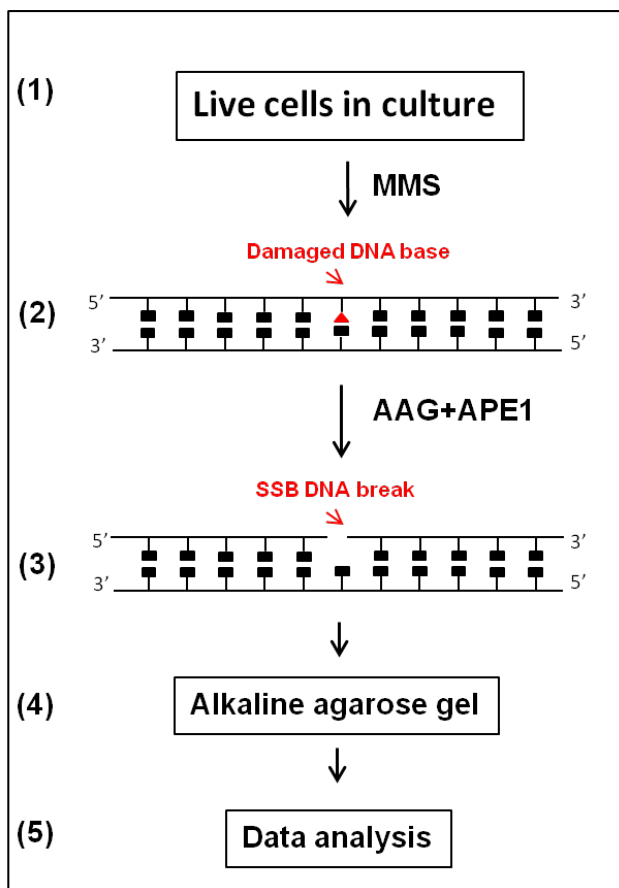
298

### 299 3. Results

300 **3.1. Alk-BER assay workflow.** The conserved nature of the BER pathway enables easy  
301 adaptation of the assay to various cell types and model organisms from lower eukaryotes to  
302 human cells. We initially developed the alk-BER assay to measure BER in yeast cells (*S.*  
303 *cerevisiae*) and successfully adapted the assay to other fungal model organism (*N. crassa*) and  
304 human cells. The alk-BER assay is based on the enzymatic conversion of the MMS-induced  
305 damaged DNA bases to single strand breaks (SSBs), which are subsequently resolved on  
306 alkaline agarose gels and quantified. The rate of BER can be analyzed by performing a DNA  
307 damage and time course for repair and assessing the rate of removal of damaged bases from  
308 the total genomic DNA. The assay is performed in 5 simple steps (**Fig. 1**) and can be completed  
309 in 3 days. The first step involves exposing the cells to sub-lethal doses of MMS to induce  
310 formation of methyl DNA adducts (mainly 7meG and 3meA). In the second step, cell aliquots  
311 corresponding with DNA damage and repair time points are collected and total genomic DNA is  
312 isolated. The third step involves conversion of MDAs to SSBs with BER enzymes (AAG  
313 glycosylase and APE1 endonuclease) that specifically bind and cleave the DNA at sites of  
314 MDAs. The fourth step involves running the samples on alkaline agarose gels to separate DNA  
315 fragments containing SSBs from the bulk genomic DNA that does not contain damage. The final  
316 step involves staining of the separated DNA fragments in the gel, acquiring an image of the gel  
317 and performing quantitation of MDAs. The alk-BER method directly quantifies the numbers of  
318 MDAs in purified genomic DNA and analyzes the kinetics of DNA repair at the whole-genome  
319 level. In order to assess the capacity of BER using the alk-BER assay, cells should be exposed  
320 to sub-lethal doses of MMS, that induce detectable levels of MDAs, but do not induce  
321 substantial cell death. To determine sub-lethal doses for specific cell line it is recommended to  
322 perform MMS dose response experiment encompassing range of MMS doses from low to high.  
323 Cell death is induced when unrepaired lesions persist due to inability of BER to efficiently repair  
324 abnormally high levels of DNA damage or when BER activity is compromised (e.g., BER gene  
325 mutants). BER capacity should also be analyzed within a specific, experimentally determined  
326 window of time following DNA damage, typically 0-3 h for yeast cells, or 0-24 h for human cells,  
327 to avoid interference from lesion bypass and DNA replication.

328

329  
330  
331  
332  
333  
334  
335  
336  
337  
338  
339  
340  
341  
342  
343  
344  
345  
346  
347



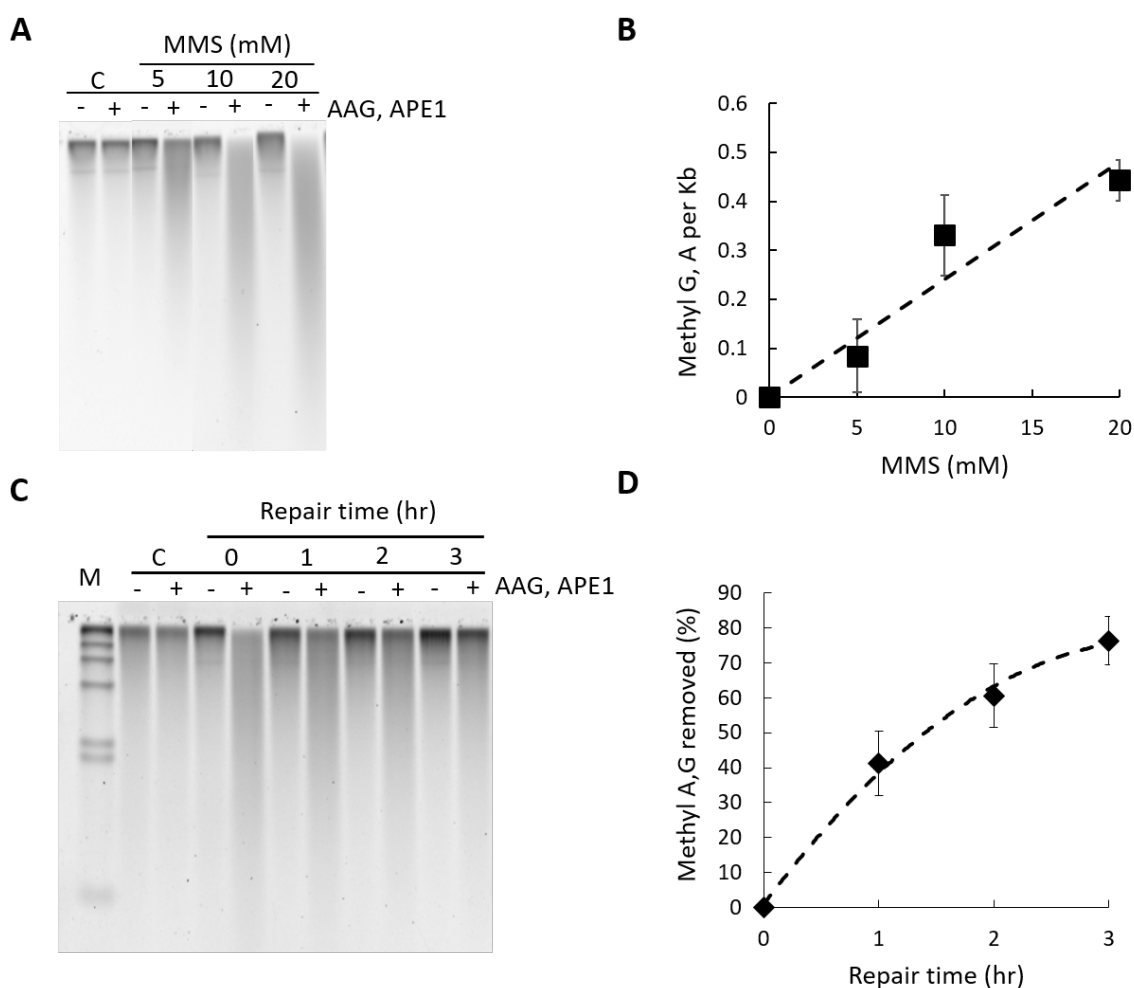
348 **Figure 1. Schematic outline of alk-BER assay.** The assay involves exposing the cells to  
349 MMS (step 1), isolation of total genomic DNA (step 2), conversion of MMS-induced methylated  
350 bases to SSBs with damage specific enzymes AAG and APE1 (step 3), separation of DNA  
351 fragments containing SSBs by alkaline agarose gel electrophoresis (step 4), gel staining,  
352 imaging, and quantitation of MDAs (step 5).

353  
354 **3.2. Alk-BER in fungal cells.** A DNA damage dose response assay was performed by  
355 exposing yeast cells (strain BY4741) to increasing doses of MMS (5, 10, 20 mM) for 10 min at  
356 30°C. Total genomic DNA was isolated and treated with AAG and APE1 enzymes. DNA  
357 samples were resolved by alkaline agarose gel electrophoresis and numbers of MDAs were  
358 quantified as described above. As the gel is run at alkaline pH, hydrogen bonding between the  
359 two DNA strands is broken to facilitate separation of strands containing breaks from non-  
360 damaged genomic DNA. The denatured DNA is maintained in a single-stranded state and  
361 migrates through the alkaline gel as a function of its size, forming a distinct smear. Increased  
362 formation of MMS-induced DNA lesions in response to increased doses of MMS is shown as

363 increases in lower molecular weight DNA molecules, also visible as a smear (**Fig. 2A**). The  
364 frequency of MDAs (7meG and 3meA) was calculated and plotted as the number of methyl A, G  
365 per kb fragment as a function of increasing doses of MMS (**Fig. 2B**). The proportional  
366 relationship between increasing MMS doses and numbers of MDAs indicates a high sensitivity  
367 of the alk-BER method, ~1.0 MDAs per 10,000 bases, that is induced by 5mM MMS dose, and  
368 ~4.0 MDAs per 10,000 bases induced by 20mM MMS in yeast cells (**Fig. 2B**).

369 DNA damage and time course of repair has been performed to evaluate the overall rate of  
370 BER to repair alkylation DNA damage in the yeast wild type strain BY4741. DNA molecules  
371 containing MMS-induced MDAs are converted to SSBs. Proficient DNA repair and restoration of  
372 genome integrity can be visually monitored as progressive shortening of the DNA smear in  
373 migration and restoration of the genome integrity by formation of high molecular weight DNA.  
374 DNA was processed with AAG and APE1 and resolved on alkaline agarose gels as described  
375 previously. A representative gel image demonstrating DNA damage and repair in the BY4741  
376 yeast strain is shown (**Fig. 2C**) and corresponding quantitative analysis of the gel is also shown  
377 (**Fig. 2D**). BER in the WT BY4741 yeast strain is proficient, and over 80% of the total MDAs in  
378 the genome are repaired after 3 h repair time at the dose used (**Fig. 2D**). The specificity of the  
379 alk-BER method was validated using yeast and *Neurospora* mutant cells deficient in BER. The  
380 yeast *mag1* $\Delta$  mutant has no Mag1 glycosylase (orthologue of human AAG) and is deficient in  
381 cleaving MMS-induced 7meG and 3meA from the DNA. Cells from the WT and *mag1* $\Delta$  strains  
382 were exposed to MMS for a total of 3 h followed by MMS removal and a 6 h-long repair time  
383 course to allow cells to repair damaged DNA. During the 3 h-long MMS exposure, mutant cells  
384 displayed higher levels of MDA formation as compared to WT because endogenous BER is  
385 inactive in the mutant cells, which results in accumulation of MDAs under the conditions of  
386 continuous MMS exposure. After removal of MMS, WT cells with proficient BER were able to  
387 clear most of the lesions during the repair time course, whereas BER-deficient *mag1* $\Delta$  cells  
388 contained high levels of unrepaired MDAs (**Fig. 3A,B,C**). The alk-BER assay was successfully  
389 adapted to multicellular fungal model *Neurospora crassa*. DNA damage and repair time course  
390 was performed with *Neurospora* WT and *mag1* $\Delta$  cells [55]. *Neurospora* cells of the wild type  
391 laboratory strain were exposed to 3.5mM MMS continuously for 3 hours, followed by repair time  
392 course in media without MMS for 5 hours. Genomic DNA was isolated and processed with  
393 combinations of AAG and APE1 enzymes and resolved on alkaline agarose gel. BER capacity  
394 to repair MMS-induced lesions in *Neurospora* cells is very efficient, with nearly complete  
395 restoration of genome integrity following 2 h repair period (**Fig.S2**).

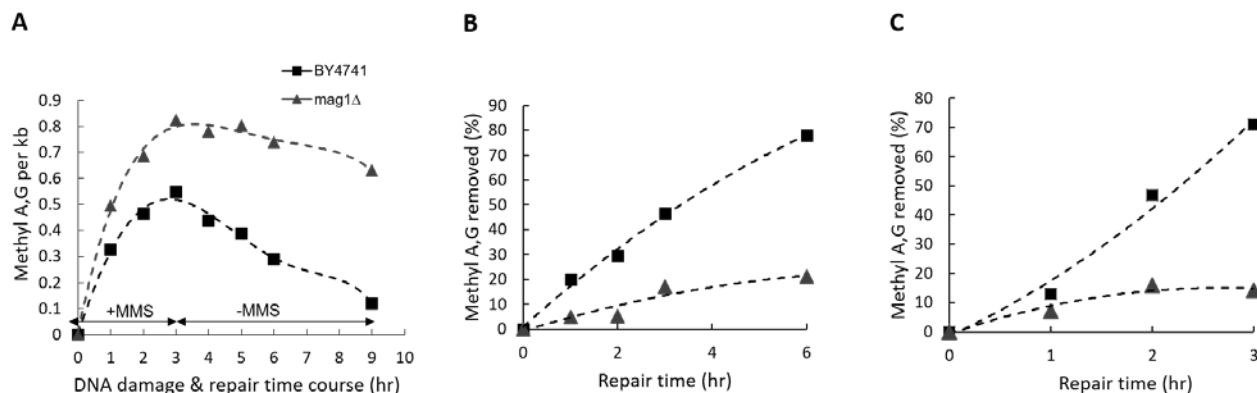
396



397

398 **Figure 2. Alk-BER assay in yeast cells (*S. cerevisiae*).** **A)** Representative alkaline agarose  
399 gel image of MMS-induced DNA damage dose response in the BY4741 strain of *S. cerevisiae*.  
400 Genomic DNA of cells not exposed to MMS (C: control), and DNA of cells exposed to increasing  
401 doses of MMS (5, 10, or 20 mM) was resolved on alkaline agarose gel. Each DNA sample was  
402 treated with (+) and without (-) a cocktail of AAG and APE1 enzymes. **B)** Dose dependent  
403 increase in the numbers of MMS-induced methyl G, A per 1 kb DNA fragment. Each data point  
404 denotes the average value and standard deviation of three independent experiments. **C)**  
405 Representative gel image of DNA damage and repair time course in the BY4741 strain of *S.*  
406 *cerevisiae*. M: DNA size standard lambda/HindIII. C: control, cells not exposed to MMS, 0: cells  
407 collected after 10 min exposure to 20 mM MMS, 1-3 h: cells collected after 1, 2, 3 h of repair.  
408 **D)** Quantitative representation of data displayed in panel C. Formation and repair of MMS-  
409 induced methyl G and A (7meG, 3meA), as a function of repair time. Each data point represents  
410 an average of 3 independent experiments; error bars were calculated based on standard

411 deviation. Gel image presented in panel A has been cropped. Uncropped gel image has been  
412 included in the supplementary data.



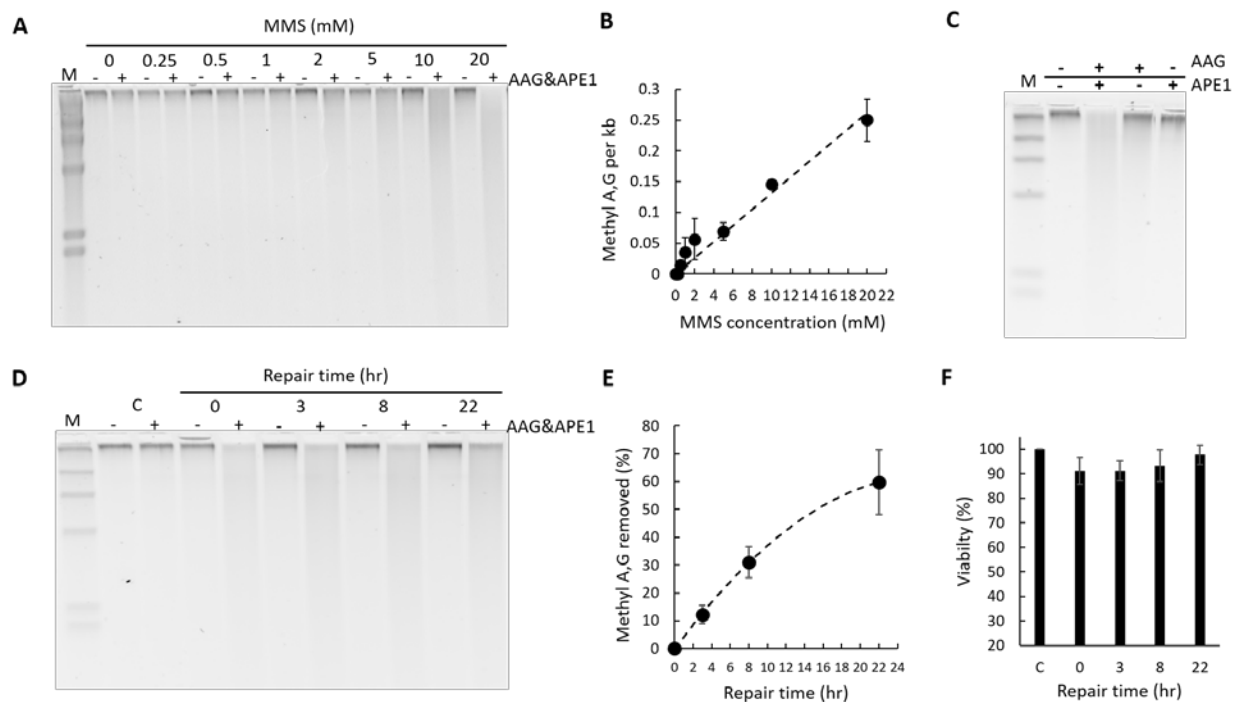
413  
414

415 **Figure 3. Alk-BER assay validation with BER-deficient yeast mutant cells, *mag1*Δ. A).** The  
416 BER rate was analyzed in *mag1*Δ mutant. WT and mutant cells were treated with 3.5mM MMS  
417 for 1- 3 h, followed by removal of media containing MMS and repair time course in fresh media  
418 for 1-6 h. **B).** Repair rates expressed as a function of % of methyl A, G removed over the repair  
419 time. **C).** Cells were treated with 20mM MMS for 10 min followed by repair time course for total  
420 of 3 hours. Repair rates expressed as a function of % of methyl A, G removed over the repair  
421 time.

422

423 **3.3. Alk-BER in human cells.** The human adrenal carcinoma SW13 cell line was used to  
424 adapt and optimize the alk-BER assay for assessing rates of BER in human cells. A series of  
425 MMS-dose response experiments were initially performed to determine the appropriate range of  
426 MMS concentration and time of the exposure for induction of detectable levels of MDAs at sub-  
427 lethal MMS doses. Cell viability was routinely monitored with trypan blue [56]. Representative  
428 MMS dose response data are presented in **Fig. 4A,B**. Increases in the smear length in  
429 response to increasing doses of MMS in the (+AAG&APE1) lanes indicate enhanced formation  
430 of MDAs. The minimal smear in (-AAG&APE1) lanes reveals formation of MDA-derived BER  
431 intermediate AP sites and SSBs that form in DNA as a result of the continuous activity of  
432 endogenous BER during MMS exposure. AP sites are fragile in alkaline conditions and can  
433 spontaneously convert to SSBs contributing to the smear in (-enzyme) lanes. The proportional  
434 relationship between increasing MMS doses and numbers of MDAs indicates a high sensitivity  
435 of the alk-BER method, ~0.7 MDAs per 10,000 bases with 5mM MMS dose in human cells.  
436 Efficiency of the individual enzymes, AAG and APE1 to convert MMS-induced MDAs to SSB in  
437 genomic DNA was assessed. We found that the cocktail of both enzymes AAG and APE1 works

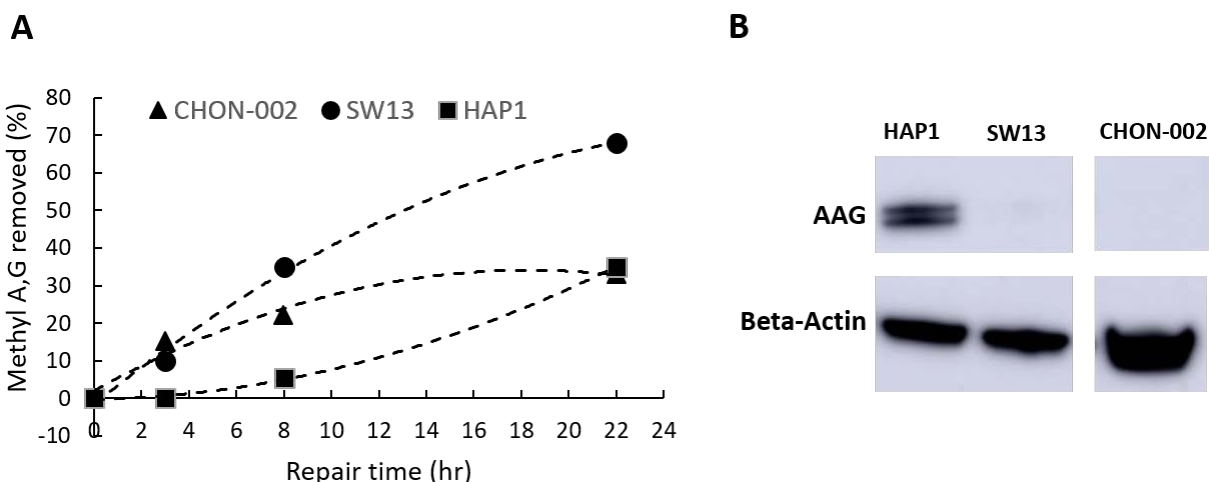
438 most efficient in converting MDAs to SSBs (**Fig. 4C**). The BER capacity in SW13 cells was  
439 analyzed by performing DNA damage and a time course of repair as described in the methods  
440 section. Cells were exposed to 10 mM MMS for 10 min in 1XPBS at RT, followed by removal of  
441 MMS and repair for 22 h in fresh media. The MMS dose used was a sublethal dose, that did not  
442 trigger significant cell death, as demonstrated by the cell viability data (**Fig. 4F**). After 22hr post  
443 MMS exposure nearly 70% of the genome was restored in SW13 cells. Representative data  
444 showing the image of the alkaline agarose gel and data quantitation are presented (**Fig. 4D,E**).  
445 Other human cell lines were subject to alk-BER assay, including untransformed fibroblast cells  
446 CHON-002, and leukemia cancer cells HAP1. The BER capacity to remove MMS-induced  
447 adducts was quantitated over distinct repair time points. The removal of MDAs appears very  
448 slow (~0-30% repair) during the first 0-8hr post MMS exposure and is consistently observed in  
449 many different human cell lines we tested. Interestingly, the repair rates vary significantly  
450 between different cell lines, and unlike in fungal cells, the rates do not appear to correlate well  
451 with the levels of AAG enzyme in the panel of cell lines we tested (**Fig.5A,B**). Additionally, alk-  
452 BER assay was performed with human lymphoblastoid cell line GM12878. Cells were exposed  
453 to 5mM MMS for 5 min, and repair rate was analyzed at 2.5 and 5 h in the repair time in media  
454 without MMS. Clearly, very slow repair was detected during the initial 5 hr repair (**Fig. S3**).  
455 Specificity of alk-BER was analyzed by exposing SW13 cells to increasing doses of oxidative  
456 agent hydrogen peroxide (H<sub>2</sub>O<sub>2</sub>), and temozolomide (TMZ), clinically used SN1 alkylator,  
457 known to induce 7meG, 3meA and O6meG adducts [57]. Exposure to H<sub>2</sub>O<sub>2</sub> does not result in  
458 formation of a dose-dependent DNA smear, indicating that alk-BER assay is specific to methyl  
459 adducts, and it cannot detect oxidative DNA damage (**Fig. S1A**). As expected, alk-BER can  
460 specifically detect TMZ-induced DNA methyl adducts in a dose dependent manner (**Fig.**  
461 **S1B,C**), although the TMZ potency to induced MDAs dose used in our experiment appears less  
462 than the potency of MMS.



463  
 464 **Figure 4. Alk-BER assay in human cells.** **A)** MMS dose response in SW13 cells. Cells were  
 465 treated with increasing doses of MMS for 10min at RT. Representative alkaline agarose gel  
 466 image is shown. **B)** Quantification of methyl A, G per 1kb DNA fragment as a function of  
 467 increasing MMS dose. The graph represents quantification of the data in panel A. **C)** Efficiency  
 468 of double enzyme (AAG&APE1), and single enzymes: (AAG only), and (APE1 only), in  
 469 converting methyl DNA adducts to SSBs. **D)** Alkaline gel image representing DNA damage and  
 470 repair time course. SW13 cells were exposed to 10mM MMS for 10min. Genomic DNA was  
 471 isolated, and processed with double enzyme AAG&APE1 digest. **E)** Quantification of the repair  
 472 and removal of methyl A, G as a function of time. **F)** SW13 cell viability measured by trypan blue.  
 473 Gel image presented in panel C has been cropped. Uncropped gel image has been included in  
 474 the supplementary data.

475  
 476





477  
478 **Figure 5. The repair of MDAs is slow in human cells and does not correlate well with the**  
479 **levels of endogenous AAG enzyme.** DNA damage and repair time course experiment was  
480 performed in several human cell lines; CHON-002, SW13, and HAP1. Cells (60-70% confluent)  
481 were exposed to 10mM (0.1%) MMS in 1xPBS for 10 min at RT, followed by DNA repair time  
482 course 0, 3, 8 and 22 hours at 37°C. **A)** DNA repair rates were quantitated individually for each  
483 cell line and expressed as a percentage (%) of the removed methyl A,G, as compared to the 0hr  
484 time point. **B)** Endogenous levels of AAG enzyme were detected by Western blotting.

485  
486

#### 487 4. Discussion

488 The efficiency of BER in repairing alkylation DNA damage varies substantially between  
489 different cells, tissues, and individuals, and has important implications in cancer development  
490 and treatment [1, 2, 58, 59]. BER efficiency is a result of a complex interplay between genetic  
491 and epigenetic factors influencing the abundance and activity of the BER enzymes, and the  
492 individual steps in the BER pathway. Ability to measure the formation and rates of repair of alkyl  
493 DNA adducts in genomic DNA provides a direct assessment of BER efficiency in a given cell  
494 type.

495 Here, we report a quantitative cell-based assay, alk-BER (alkylation Base Excision Repair),  
496 adapted and optimized for measuring efficiency and rates of BER following alkylation DNA  
497 damage in fungal model organisms (*S.cerevisiae*, *N.crassa*) and human cell lines (SW13,  
498 CHON-002, HAP1 and GM12878). Alk-BER offers a simple, time- and cost-efficient, cell-based  
499 method for quantitative analysis of alkylation DNA damage and repair in the genomic DNA. The

500 alk-BER assay can be used to determine BER efficiency in various cell types, by assessment of  
501 the rates of methyl DNA adducts removal from the DNA over time.

502 Yeast cells have been extensively used to study DNA repair processes in eukaryotic cells  
503 [60]. Yeast have a robust and conserved BER pathway to repair alkylation DNA damage. Using  
504 alk-BER assay, we found that in wild type strains of fungal model organisms (*S. cerevisiae* and  
505 *N. crassa*), BER proceeds quite rapidly, following removal of the MMS from the growth media.  
506 We showed that BER in the BY4741 strain of *S. cerevisiae* is nearly completed within 3-4 h post  
507 exposure since nearly 80-90% of the lesions were removed from the genome (**Fig. 2C, D**).  
508 Similarly, repair of alkylation DNA damage has been nearly completed within 2-4 h in the wild  
509 type laboratory strain of *N. crassa* [55] (**Fig.S2**). We also showed that BER-deficient *mag1Δ*  
510 yeast mutant cells were deficient to clear MMS-induced lesions and accumulated MDAs over  
511 time, which validates specificity of the alk-BER assay (**Fig. 3A,B,C**). The human genome is  
512 much larger therefore repair is expected to take longer compared to lower eukaryotes. We  
513 found that the majority of the genome (~70% lesions removed) was restored following 22 h post  
514 MMS exposure in SW13 cells (**Fig. 4D,E, 5A**), which is consistent with previous studies  
515 reporting that majority of DNA alkylation repair in mammalian cells can be completed within 24 h  
516 post exposure, as revealed by results generated with various quantification methods [39, 61-65].  
517 We found that the rates of BER to remove MMS-induced DNA adducts vary significantly  
518 between SW13 and CHON-002, and HAP1 cell lines and do not correlate well with the  
519 endogenous levels of AAG enzyme in these cell lines (**Fig. 5A,B**). These rates can be  
520 influenced by the endogenous levels and activities of various BER enzymes, including additional  
521 glycosylases, and other regulators of DNA repair. Future studies are needed to further  
522 investigate the mechanisms and regulators of DNA alkylation repair in human cells.

523 In lower eukaryotes (*S.cerevisiae*, *N.crassa*), the rate of repair of MMS-induced methyl DNA  
524 adducts is strongly dependent on the functional MAG1 glycosylase, where *mag1Δ* mutants  
525 demonstrate abolished ability to repair MDAs. Interestingly, repair of MDAs in certain  
526 mammalian cells does not appear to be exclusively dependent on AAG glycosylase. It has been  
527 reported that the alkylated bases 3meA and 7meG, both AAG substrates generated from MMS  
528 treatment, are removed from the genome of AAG-deficient embryonic stem cells, with slower  
529 kinetics for 3meA but comparable kinetics for 7meG [66]. Other study revealed that similar  
530 levels of 7meG were detected in livers of AAG<sup>+/+</sup> and AAG<sup>-/-</sup> mice 24hr after exposure to MNU  
531 [67]. These studies suggest that in mammalian cells methyl DNA adducts can be excised and  
532 repaired in the absence of AAG enzyme, perhaps by involvement of other glycosylases, or

533 spontaneous depurination. Future application of alk-BER could facilitate further understanding  
534 of the role of AAG and other factors in regulation of human BER.

535 The alk-BER could serve as useful framework for number of approaches to study repair of  
536 DNA alkylation. For example, alk-BER assay could be used to distinguish, in a quantitative way,  
537 between the levels of MDAs and levels of downstream repair intermediates, such as AP sites.  
538 Highly specific and sensitive detection of AP sites could also be performed by processing of the  
539 sample with the AAG enzyme only (converts MDA to AP sites) and subsequent detection of AP  
540 sites using a highly sensitive AP site detection kit (e.g., Abcam, ab 211154). Alk-BER assay can  
541 also serve as a framework for quantification of gene-specific repair when coupled with Southern  
542 blot and hybridization of gene-specific probes. Alk-BER could also be useful in detection and  
543 quantification of MMS-induced methyl DNA adducts in preparation and optimization of samples  
544 for the approaches involving next generation sequencing, such as NMP-seq.

545 In summary, the alk-BER assay offers a versatile, reliable and affordable approach for  
546 quantitative analysis of DNA damage formation and repair following exposure to DNA  
547 methylating alkylating agents. The alk-BER assay can be easily optimized to be used in any  
548 type of cultured cells, and integrated with the existing approaches to study mechanisms  
549 regulating BER balance and capacity. The assay has the ability to detect imbalances in the  
550 activity of the BER process, that is highly relevant to cancer development and treatment.  
551 Quantitative analyses of DNA alkylation damage and repair using fungal genetic model  
552 organisms and human cell lines offer unique opportunities to identify novel, conserved  
553 regulators of BER.

554

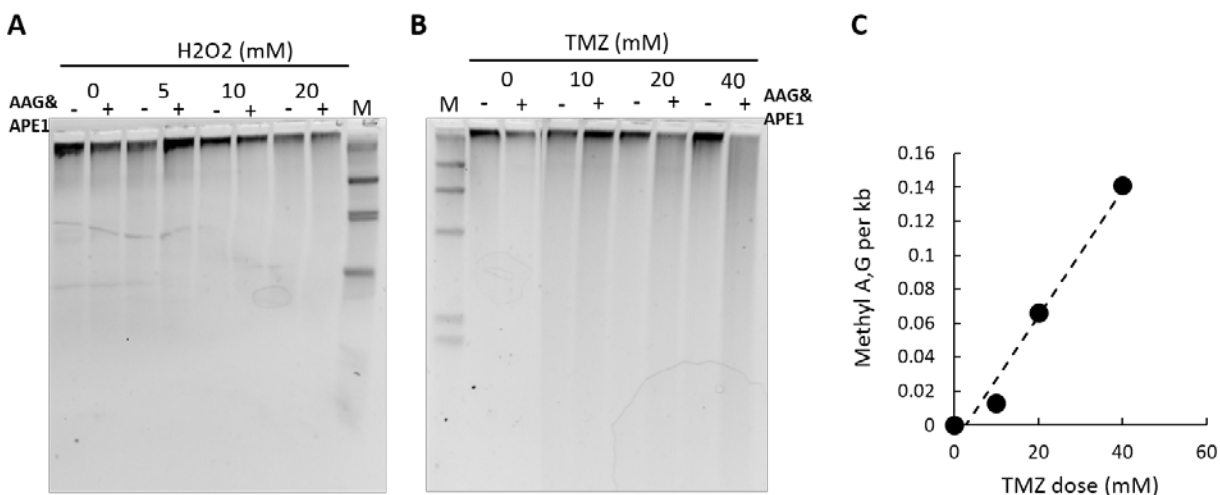
## 555 **Acknowledgements**

556 We thank Dr. Ann Bode for help with proof reading the manuscript. We would like to  
557 acknowledge Dr. John Wyrick for helpful discussions and intellectual contributions to this work.  
558 This work was supported by grant R01ES002614 from the National Institute of Environmental  
559 Health Sciences (NIEHS) (to M.J.S. and J.J.W.), R21ES028549 from NIEHS to W.C., and  
560 Faculty Research Grant from University of Georgia to W.C. The contents are solely the  
561 responsibility of the authors and do not necessarily represent the official views of the NIEHS,  
562 NIH.

563

564

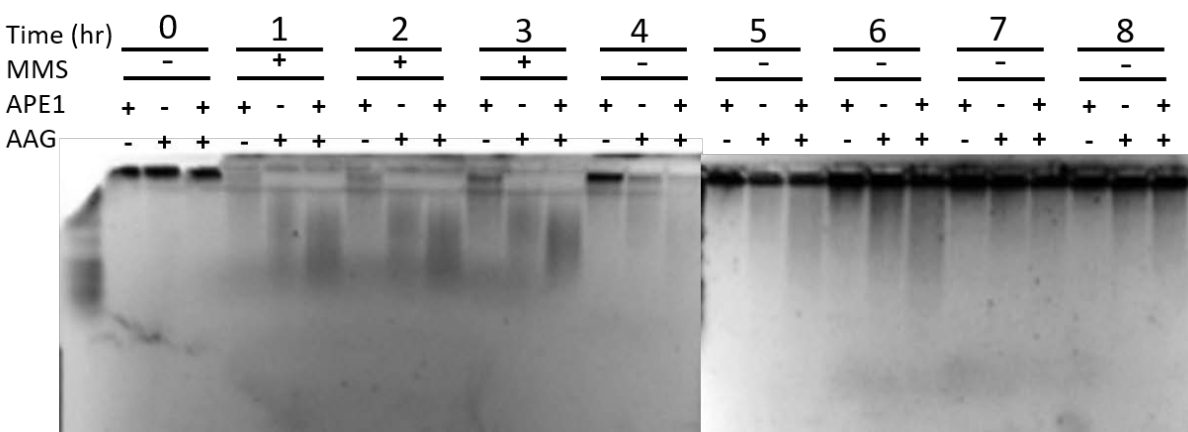
565 **Supplementary Information**



566

567 **Figure S1. Specificity of alk-BER.** **A)** Hydrogen peroxide (H<sub>2</sub>O<sub>2</sub>) induced DNA damage.  
 568 SW13 cells were exposed to increasing doses of H<sub>2</sub>O<sub>2</sub> for 5min at RT, followed by DNA  
 569 purification, AAG&APE1 digest and alkaline agarose gel electrophoresis. **B)** Temozolomide  
 570 (TMZ) induced DNA damage. SW13 cells were exposed to increasing doses of TMZ for 10 min  
 571 at RT, followed by DNA purification, AAG&APE1 digest and alkaline agarose gel electrophoresis  
 572 and data quantification. **C)** Quantification data of TMZ dose dependent accumulation of methyl  
 573 A,G per kb DNA fragment.

574



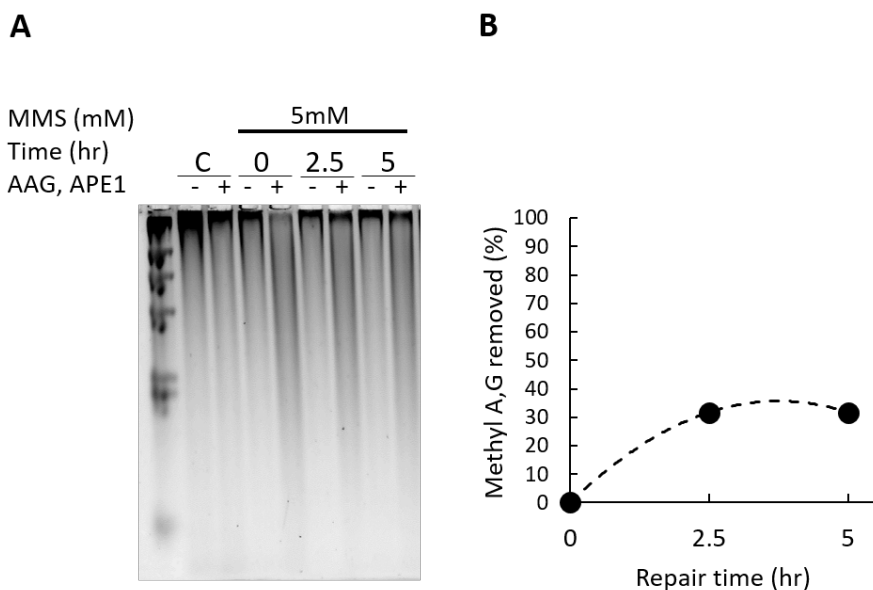
575

**Figure S2. Alk-BER assay in *Neurospora crassa*.** Representative alkaline agarose gel image of MMS-induced DNA damage, followed by DNA repair in the wild type strain of *Neurospora*, 0: control genomic DNA from cells not exposed to MMS; 1-3 hours: DNA from cells exposed to 3.5mM MMS continuously for 1, 2 and 3 hours respectively; 4-8 hours: DNA from cells that were allowed to repair DNA in media without MMS for 1-4 hours respectively. Each DNA sample was treated with combination of human APE1 and AAG enzymes: APE1 (+) and without AAG (-), without APE1 (-) and with AAG (+), and with both enzymes APE (+) & AAG (+).

576

577

578



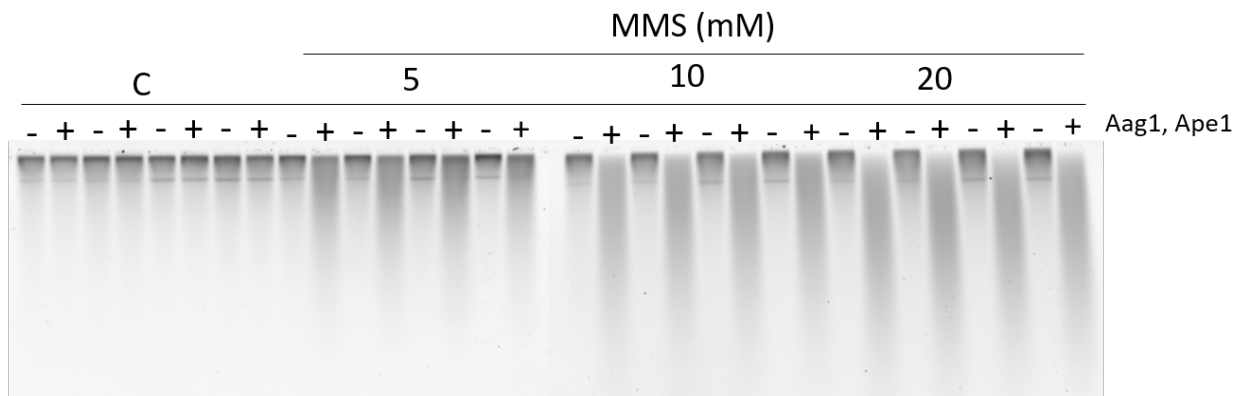
579

580

581 **Figure S3. Alk-BER assay in human lymphoblastoid cell line GM12878.** The representative  
 582 alkaline agarose gel illustrates DNA damage and repair time course performed with GM12878  
 583 cells. Cells were treated with 5mM MMS for 5 minutes, MMS was removed and cells were  
 584 allowed to repair DNA for 2.5 and 5 hours.

585 **Uncropped gel images**

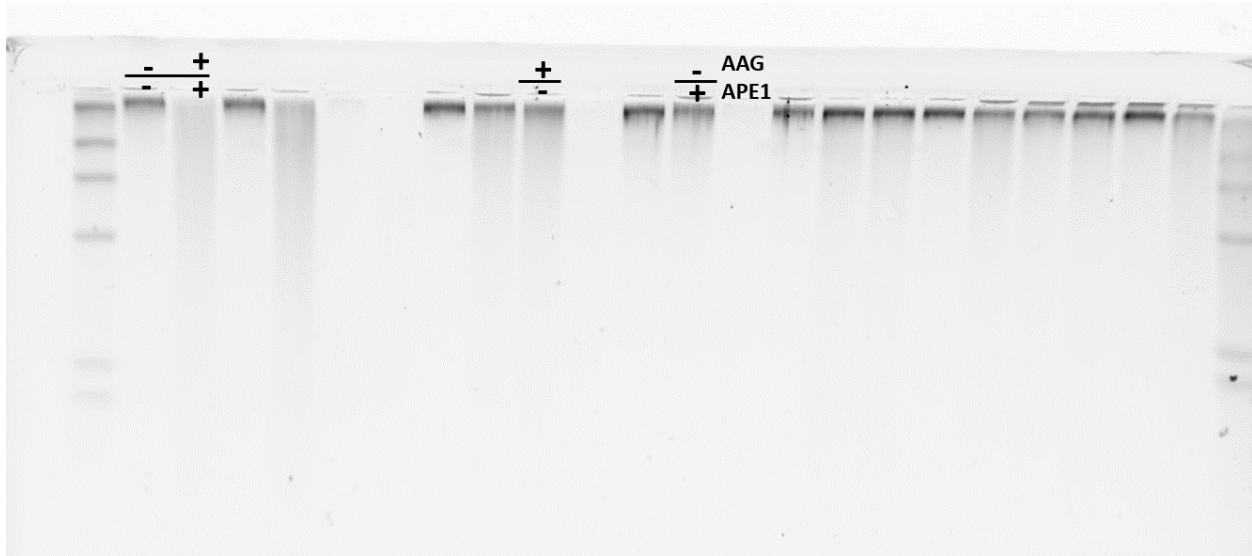
586 **Uncropped gel image for Figure 2A.**



587

588

589 **Uncropped gel image Figure 4C.**



590

591

## 592 References

593

594 1. Beranek, D.T., *Distribution of methyl and ethyl adducts following alkylation with*  
595 *monofunctional alkylating agents*. Mutat Res, 1990. **231**(1): p. 11-30.

596 2. Fu, D., J.A. Calvo, and L.D. Samson, *Balancing repair and tolerance of DNA damage*  
597 *caused by alkylating agents*. Nat Rev Cancer, 2012. **12**(2): p. 104-20.

598 3. Margison, G.P., M.F. Santibanez Koref, and A.C. Povey, *Mechanisms of*  
599 *carcinogenicity/chemotherapy by O6-methylguanine*. Mutagenesis, 2002. **17**(6): p. 483-  
600 7.

601 4. Saffhill, R., G.P. Margison, and P.J. O'Connor, *Mechanisms of carcinogenesis induced*  
602 *by alkylating agents*. Biochim Biophys Acta, 1985. **823**(2): p. 111-45.

603 5. Klapacz, J., et al., *Frameshift mutagenesis and microsatellite instability induced by*  
604 *human alkyladenine DNA glycosylase*. Mol Cell, 2010. **37**(6): p. 843-53.

605 6. Pfeifer, G.P., et al., *Tobacco smoke carcinogens, DNA damage and p53 mutations in*  
606 *smoking-associated cancers*. Oncogene, 2002. **21**(48): p. 7435-51.

607 7. Richardson, F.C. and K.K. Richardson, *Sequence-dependent formation of alkyl DNA*  
608 *adducts: a review of methods, results, and biological correlates*. Mutat Res, 1990. **233**(1-  
609 2): p. 127-38.

610 8. Head, R.J., et al., *Persistence of DNA adducts, hypermutation and acquisition of cellular*  
611 *resistance to alkylating agents in glioblastoma*. Cancer Biol Ther, 2017: p. 0.

612 9. McNERNEY, M.E., L.A. Godley, and M.M. Le Beau, *Therapy-related myeloid neoplasms:*  
613 *when genetics and environment collide*. Nat Rev Cancer, 2017. **17**(9): p. 513-527.

614 10. Chaim, I.A., et al., *In vivo measurements of interindividual differences in DNA*  
615 *glycosylases and APE1 activities*. Proc Natl Acad Sci U S A, 2017.

616 11. Nagel, Z.D., I.A. Chaim, and L.D. Samson, *Inter-individual variation in DNA repair*  
617 *capacity: a need for multi-pathway functional assays to promote translational DNA repair*  
618 *research*. DNA Repair (Amst), 2014. **19**: p. 199-213.

619 12. Chatterjee, N. and G.C. Walker, *Mechanisms of DNA damage, repair, and mutagenesis*.  
620 Environ Mol Mutagen, 2017. **58**(5): p. 235-263.

621 13. Soll, J.M., R.W. Sobol, and N. Mosammamarast, *Regulation of DNA Alkylation Damage*  
622 *Repair: Lessons and Therapeutic Opportunities*. Trends Biochem Sci, 2017. **42**(3): p.  
623 206-218.

624 14. Kim, Y.J. and D.M. Wilson, 3rd, *Overview of base excision repair biochemistry*. Curr Mol  
625 Pharmacol, 2012. **5**(1): p. 3-13.

626 15. Samson, L., et al., *Cloning and characterization of a 3-methyladenine DNA glycosylase*  
627 *cDNA from human cells whose gene maps to chromosome 16*. Proc Natl Acad Sci U S  
628 A, 1991. **88**(20): p. 9127-31.

629 16. Samson, L.D., *The repair of DNA alkylation damage by methyltransferases and*  
630 *glycosylases*. Essays Biochem, 1992. **27**: p. 69-78.

631 17. Li, M. and D.M. Wilson, 3rd, *Human apurinic/aprimidinic endonuclease 1*. Antioxid  
632 Redox Signal, 2014. **20**(4): p. 678-707.

633 18. Wilson, D.M., 3rd, M. Takeshita, and B. Demple, *Abasic site binding by the human*  
634 *apurinic endonuclease, Ape, and determination of the DNA contact sites*. Nucleic Acids  
635 Res, 1997. **25**(5): p. 933-9.

636 19. Ko, H.L. and E.C. Ren, *Functional Aspects of PARP1 in DNA Repair and Transcription*.  
637 Biomolecules, 2012. **2**(4): p. 524-48.

638 20. Wei, H. and X. Yu, *Functions of PARylation in DNA Damage Repair Pathways*.  
639 Genomics Proteomics Bioinformatics, 2016. **14**(3): p. 131-139.

- 640 21. Wilson, S.H., et al., *DNA polymerase beta and mammalian base excision repair*. Cold  
641 Spring Harb Symp Quant Biol, 2000. **65**: p. 143-55.
- 642 22. Tomkinson, A.E. and Z.B. Mackey, *Structure and function of mammalian DNA ligases*.  
643 Mutat Res, 1998. **407**(1): p. 1-9.
- 644 23. Tomkinson, A.E. and A. Sallmyr, *Structure and function of the DNA ligases encoded by*  
645 *the mammalian LIG3 gene*. Gene, 2013. **531**(2): p. 150-7.
- 646 24. Ensminger, M., et al., *DNA breaks and chromosomal aberrations arise when replication*  
647 *meets base excision repair*. J Cell Biol, 2014. **206**(1): p. 29-43.
- 648 25. Calvo, J.A., et al., *Aag DNA glycosylase promotes alkylation-induced tissue damage*  
649 *mediated by Parp1*. PLoS Genet, 2013. **9**(4): p. e1003413.
- 650 26. Ebrahimkhani, M.R., et al., *Aag-initiated base excision repair promotes ischemia*  
651 *reperfusion injury in liver, brain, and kidney*. Proc Natl Acad Sci U S A, 2014. **111**(45): p.  
652 E4878-86.
- 653 27. Meira, L.B., et al., *Aag-initiated base excision repair drives alkylation-induced retinal*  
654 *degeneration in mice*. Proc Natl Acad Sci U S A, 2009. **106**(3): p. 888-93.
- 655 28. Redaelli, A., et al., *AP endonuclease activity in humans: development of a simple assay*  
656 *and analysis of ten normal individuals*. Teratog Carcinog Mutagen, 1998. **18**(1): p. 17-26.
- 657 29. Brennerman, B.M., J.L. Illuzzi, and D.M. Wilson, 3rd, *Base excision repair capacity in*  
658 *informing healthspan*. Carcinogenesis, 2014. **35**(12): p. 2643-52.
- 659 30. Memisoglu, A.S., L., *Base excision repair in yeast and mammals*. Mutation Research,  
660 2000. **451**: p. 39-51.
- 661 31. Wallace, S.S., *Base excision repair: a critical player in many games*. DNA Repair (Amst),  
662 2014. **19**: p. 14-26.
- 663 32. Wallace, S.S., D.L. Murphy, and J.B. Sweasy, *Base excision repair and cancer*. Cancer  
664 Lett, 2012. **327**(1-2): p. 73-89.
- 665 33. Abbotts, R., N. Thompson, and S. Madhusudan, *DNA repair in cancer: emerging targets*  
666 *for personalized therapy*. Cancer Manag Res, 2014. **6**: p. 77-92.
- 667 34. Montaldi, A.P., P.R. Godoy, and E.T. Sakamoto-Hojo, *APE1/REF-1 down-regulation*  
668 *enhances the cytotoxic effects of temozolomide in a resistant glioblastoma cell line*.  
669 Mutat Res Genet Toxicol Environ Mutagen, 2015. **793**: p. 19-29.
- 670 35. Montaldi, A.P. and E.T. Sakamoto-Hojo, *Methoxyamine sensitizes the resistant*  
671 *glioblastoma T98G cell line to the alkylating agent temozolomide*. Clin Exp Med, 2013.  
672 **13**(4): p. 279-88.
- 673 36. Sultana, R., et al., *Synthetic lethal targeting of DNA double-strand break repair deficient*  
674 *cells by human apurinic/apyrimidinic endonuclease inhibitors*. Int J Cancer, 2012.  
675 **131**(10): p. 2433-44.
- 676 37. Liu, L., Y. Nakatsuru, and S.L. Gerson, *Base excision repair as a therapeutic target in*  
677 *colon cancer*. Clin Cancer Res, 2002. **8**(9): p. 2985-91.
- 678 38. Guo, J. and R.J. Turesky, *Emerging Technologies in Mass Spectrometry-Based DNA*  
679 *Adductomics*. High Throughput, 2019. **8**(2).
- 680 39. Haque, K., et al., *Accurate and sensitive quantitation of N7-methyldeoxyguanosine-3'-*  
681 *monophosphate by <sup>32</sup>P-postlabeling and storage-phosphor imaging*. Chem Res Toxicol,  
682 1997. **10**(6): p. 660-6.
- 683 40. Liu, S. and Y. Wang, *Mass spectrometry for the assessment of the occurrence and*  
684 *biological consequences of DNA adducts*. Chem Soc Rev, 2015. **44**(21): p. 7829-54.
- 685 41. Thomas, B., et al., *A novel method for detecting 7-methyl guanine reveals aberrant*  
686 *methylation levels in Huntington disease*. Anal Biochem, 2013. **436**(2): p. 112-20.
- 687 42. Fortini, P., et al., *Analysis of DNA alkylation damage and repair in mammalian cells by*  
688 *the comet assay*. Mutagenesis, 1996. **11**(2): p. 169-75.
- 689 43. Hartmann, A., et al., *Recommendations for conducting the in vivo alkaline Comet assay.*  
690 *4th International Comet Assay Workshop*. Mutagenesis, 2003. **18**(1): p. 45-51.



- 691 44. Alanazi, J.S. and J.J. Latimer, *Host Cell Reactivation: Assay for Actively Transcribed*  
692 *DNA (Nucleotide Excision) Repair Using Luciferase Family Expression Vectors*. *Methods*  
693 *Mol Biol*, 2020. **2102**: p. 509-528.
- 694 45. Wang, L., et al., *A modified host-cell reactivation assay to measure repair of alkylating*  
695 *DNA damage for assessing risk of lung adenocarcinoma*. *Carcinogenesis*, 2007. **28**(7):  
696 p. 1430-6.
- 697 46. Li, M., T. Ko, and S. Li, *High-resolution Digital Mapping of N-Methylpurines in Human*  
698 *Cells Reveals Modulation of Their Induction and Repair by Nearest-neighbor*  
699 *Nucleotides*. *J Biol Chem*, 2015. **290**(38): p. 23148-61.
- 700 47. Mao, P., et al., *Genome-wide maps of alkylation damage, repair, and mutagenesis in*  
701 *yeast reveal mechanisms of mutational heterogeneity*. *Genome Res*, 2017. **27**(10): p.  
702 1674-1684.
- 703 48. Sutherland, B.M., P.V. Bennett, and J.C. Sutherland, *DNA damage quantitation by*  
704 *alkaline gel electrophoresis*. *Methods Mol Biol*, 2006. **314**: p. 251-73.
- 705 49. Czaja, W., et al., *Proficient repair in chromatin remodeling defective ino80 mutants of*  
706 *Saccharomyces cerevisiae highlights replication defects as the main contributor to DNA*  
707 *damage sensitivity*. *DNA Repair (Amst)*, 2010. **9**(9): p. 976-84.
- 708 50. Czaja, W., P. Mao, and M.J. Smerdon, *Chromatin remodelling complex RSC promotes*  
709 *base excision repair in chromatin of Saccharomyces cerevisiae*. *DNA Repair (Amst)*,  
710 2014. **16**: p. 35-43.
- 711 51. Bepalov, V.A., et al., *Improved method for measuring the ensemble average of strand*  
712 *breaks in genomic DNA*. *Environ Mol Mutagen*, 2001. **38**(2-3): p. 166-74.
- 713 52. Alseth, I., et al., *Biochemical characterization and DNA repair pathway interactions of*  
714 *Mag1-mediated base excision repair in Schizosaccharomyces pombe*. *Nucleic Acids*  
715 *Res*, 2005. **33**(3): p. 1123-31.
- 716 53. Sambrook, J. and D.W. Russell, *Alkaline agarose gel electrophoresis*. *CSH Protoc*,  
717 2006. **2006**(1).
- 718 54. Veatch, W. and S. Okada, *Radiation-induced breaks of DNA in cultured mammalian*  
719 *cells*. *Biophys J*, 1969. **9**(3): p. 330-46.
- 720 55. Basenko, E.Y., et al., *The LSH/DDM1 Homolog MUS-30 Is Required for Genome*  
721 *Stability, but Not for DNA Methylation in Neurospora crassa*. *PLoS Genet*, 2016. **12**(1):  
722 p. e1005790.
- 723 56. Strober, W., *Trypan Blue Exclusion Test of Cell Viability*. *Curr Protoc Immunol*, 2015.  
724 **111**: p. A3 B 1-A3 B 3.
- 725 57. Trivedi, R.N., et al., *The role of base excision repair in the sensitivity and resistance to*  
726 *temozolomide-mediated cell death*. *Cancer Res*, 2005. **65**(14): p. 6394-400.
- 727 58. Dianov, G.L., *Base excision repair targets for cancer therapy*. *Am J Cancer Res*, 2011.  
728 **7**(1): p. 845-851.
- 729 59. Dianov, G.L. and U. Hubscher, *Mammalian base excision repair: the forgotten*  
730 *archangel*. *Nucleic Acids Res*, 2013. **41**(6): p. 3483-90.
- 731 60. Boiteux, S. and S. Jinks-Robertson, *DNA repair mechanisms and the bypass of DNA*  
732 *damage in Saccharomyces cerevisiae*. *Genetics*, 2013. **193**(4): p. 1025-64.
- 733 61. Fortini, P., *The base excision repair: mechanisms and its relevance for cancer*  
734 *susceptibility*. *Biochimie*, 2003. **85**(11): p. 1053-1071.
- 735 62. Lawley, P.D., et al., *Repair of chemical carcinogen-induced damage in DNA of human*  
736 *lymphocytes and lymphoid cell lines--studies of the kinetics of removal of O6-*  
737 *methylguanine and 3-methyladenine*. *Chem Biol Interact*, 1986. **57**(1): p. 107-21.
- 738 63. Scicchitano, D.A. and P.C. Hanawalt, *Repair of N-methylpurines in specific DNA*  
739 *sequences in Chinese hamster ovary cells: absence of strand specificity in the*  
740 *dihydrofolate reductase gene*. *Proc Natl Acad Sci U S A*, 1989. **86**(9): p. 3050-4.

- 741 64. Wang, W., A. Sitaram, and D.A. Scicchitano, *3-Methyladenine and 7-methylguanine*  
742 *exhibit no preferential removal from the transcribed strand of the dihydrofolate reductase*  
743 *gene in Chinese hamster ovary B11 cells*. *Biochemistry*, 1995. **34**(5): p. 1798-804.
- 744 65. Ye, N., G.P. Holmquist, and T.R. O'Connor, *Heterogeneous repair of N-methylpurines at*  
745 *the nucleotide level in normal human cells*. *J Mol Biol*, 1998. **284**(2): p. 269-85.
- 746 66. Smith, S.A. and B.P. Engelward, *In vivo repair of methylation damage in Aag 3-*  
747 *methyladenine DNA glycosylase null mouse cells*. *Nucleic Acids Res*, 2000. **28**(17): p.  
748 3294-300.
- 749 67. Elder, R.H., et al., *Alkylpurine-DNA-N-glycosylase knockout mice show increased*  
750 *susceptibility to induction of mutations by methyl methanesulfonate*. *Mol Cell Biol*, 1998.  
751 **18**(10): p. 5828-37.

752

753

#### 754 **Author Statement**

755 Conceptualization: Wioletta Czaja, Peng Mao, Michael Smerdon. Funding acquisition: Wioletta  
756 Czaja, Michael Smerdon. Investigation: Wioletta Czaja, Yong Li, Peng Mao, Evelina Y.  
757 Basenko. Validation: Wioletta Czaja, Yong Li. Methodology: Wioletta Czaja, Peng Mao, Michael  
758 Smerdon. Project administration: Wioletta Czaja. Resources: Wioletta Czaja, Michael Smerdon,  
759 Zachary Lewis. Supervision: Wioletta Czaja, Michael Smerdon, Zachary Lewis. Visualization:  
760 Wioletta Czaja. Writing-Original Draft: Wioletta Czaja. Writing – review & editing: Wioletta Czaja,  
761 Michael Smerdon, Peng Mao.

#### 762 **Additional Information**

#### 763 **Competing Interests**

764 None

765 We know of no conflicts of interest associated with this manuscript, and there has been no  
766 significant financial support for this work that could have influenced its outcome.

767